iScience, Volume *23*

Supplemental Information

Low Shear Stress Increases Recombinant Protein Production and High Shear Stress Increases Apoptosis in Human Cells

Caijuan Zhan, Gholamreza Bidkhori, Hubert Schwarz, Magdalena Malm, Aman Mebrahtu, Ray Field, Christopher Sellick, Diane Hatton, Paul Varley, Adil Mardinoglu, Johan Rockberg, and Veronique Chotteau

Figure S.1 - Evolution of the Reynolds number, the shear rate (A) and the shear stress (B) as function of different flow rates in the hollow fiber of a tangential flow filtration cartridge - Related to Section Theoretical considerations - Shear stress characterization, to Figure 1 and to Transparent Methods – A.1 Shear stress characterization: Velocity profile during one cycle in ATF (C). Shear rate (D) and shear stress (E) for ATF and TFF modes of operation as function of the flow rate

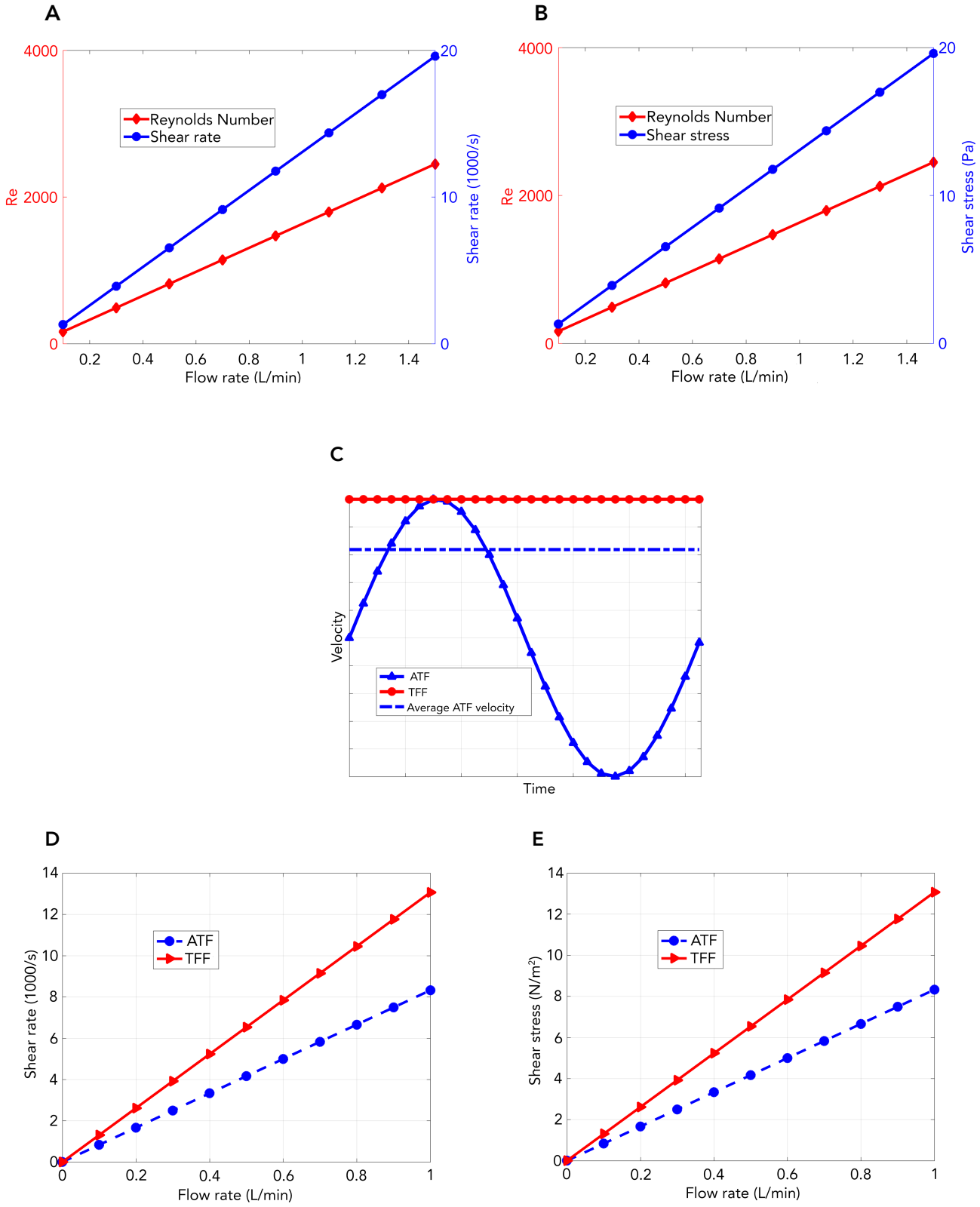

Figure S.2 - EDR (energy dissipation rate) generated from the passage in the hollow fiber lumen of a hollow fiber cartridge CFP-4-E-3MA of 13 fibers and fiber lumen of 1 mm (GE Healthcare), used in the present study - Related to Section Discussion, to Figure 7 and to Transparent Methods – A.2 Energy dissipation rate: (A) along the radius of the hollow fibers for three different flow rates, starting from the lumen center; (B) maximal EDR as function of the flow rate

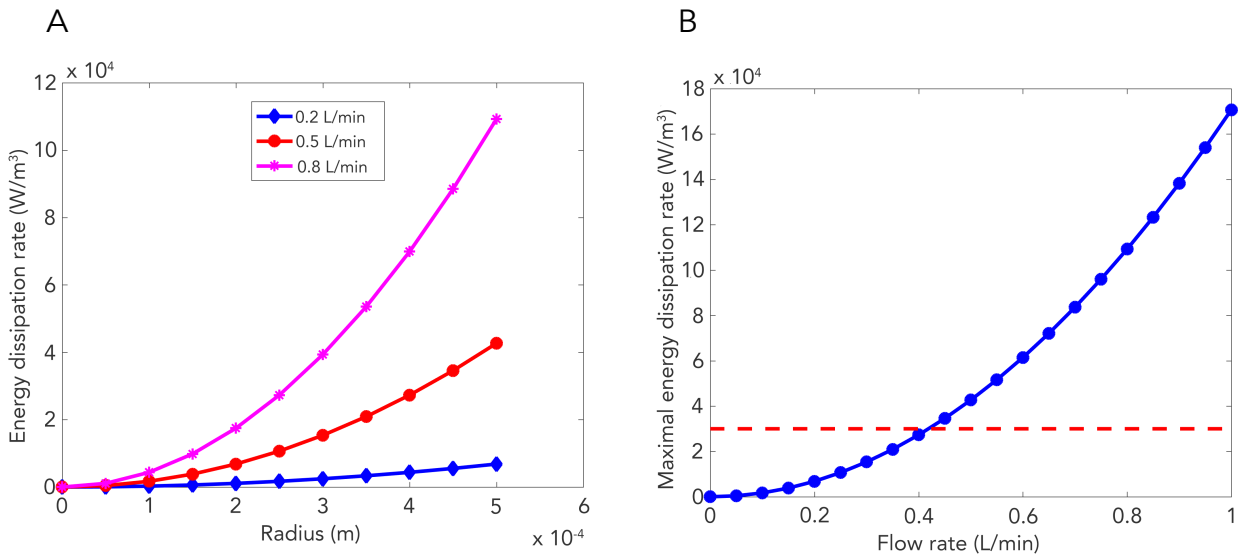

Figure S.3 – Relation between the relative cell specific amino acid consumption rate and the shear rate in TFF and ATF; relative amino acid consumption with respect to amino acid consumption in control 'No shear' (in absence of shear stress) - Related to Section Shear stress-related cytoskeleton/cell adhesion reorganization and cell death and Figure 4

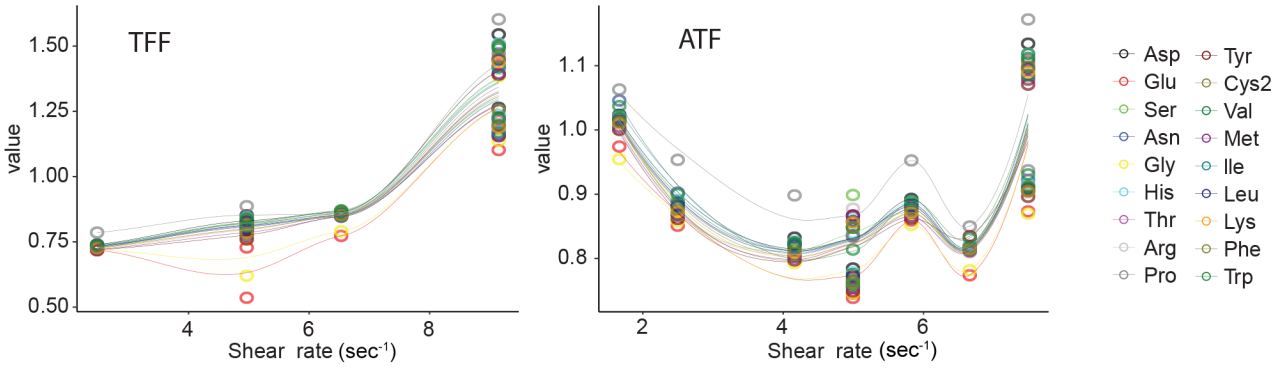

KEY RESOURCES TABLE

REAGENT or RESOURCE	SOURCE	IDENTIFIER
Antibodies		
CaptureSelect Biotin Anti-EPO Conjugate	Thermo Fisher Scientific	7103372500
Chemicals, Peptides, and Recombinant Proteins		
CD-optiCHO medium	Thermo Fisher Scientific	Cat No. 12681011
Puromycin dihydrochloride	Thermo Fisher Scientific	Cat No. A1113803
RNAlater stabilization solution	Thermo Fisher Scientific	Cat No. AM7021
Experimental Models: Cell Lines		
Human: Freestyle 293-F	Thermo Fisher Scientific	R79007
Freestyle 293-F: HEK293: EPO-HPC4-GFP11	This paper	N/A
Recombinant DNA		
pD2529-CMV	Atum	pD2529-CMV
Software and Algorithms		
PathWave	Schramm 2010	https://github.com/KoenigLabNM/Pathwave
Cytoscape	Shannon 2003	https://cytoscape.org/
PIANO	Väremo 2013	https://bioconductor.org/packages/release/bioc/html/piano.html
MSigDB	Liberzon 2015	https://www.gsea-msigdb.org/gsea/msigdb
DESeq2	Love 2014	https://bioconductor.org/packages/release/bioc/html/DESeq2.html
Kallisto	Bray 2016	https://pachterlab.github.io/kallisto/about
org.Hs.eg.db	Carlson 2019	https://bioconductor.org/packages/release/data/annotation/html/org.Hs.eg.db.html
Other		
Microfiltration hollow fiber cartridge	GE Healthcare - Cytiva	CFP-4-E-3MA

TRANSPARENT METHODS

A THEORETICAL CONSIDERATIONS

A.1 Shear stress characterization

The flow in a hollow fiber cartridge at steady state has a Poiseuille profile, i.e. the cross-section velocity has a parabolic profile. The Reynolds number, Re, can be used to predict if a flow is laminar or turbulent inside a hollow fiber.

$$Re = u\frac{L}{\nu} \tag{S.1}$$

where u is the velocity of the fluid (m/s), L is the hydraulic diameter (m) and ν is the kinematic viscosity of the fluid (m^2/s). The shear rate and shear stress in the hollow fiber can be calculated as follows

$$\gamma = \frac{\partial u}{\partial y} \tag{S.2}$$

$$\tau = \sigma\ \frac{\partial u}{\partial y} = \sigma\ \gamma \tag{S.3}$$

where γ is the shear rate, τ is the shear stress, σ is the dynamic viscosity of the fluid and $\nu = {}^{\sigma}/_{\rho}$, where ρ is the fluid density. In a pipe the shear rate is given by

$$\gamma = \frac{4\ Q_{fiber}}{\Pi\ R^3} \tag{S.4}$$

where Q_{fiber} is the flow rate in a fiber and R is the fiber radius (Selection Handbook, Cross Flow Filtration Method Handbook).

Using **Eq**. S.8 and S.9, the shear rate and shear stress were calculated for the present hollow fiber cartridge (see Material and Method) and given in Figure S.1D-E. The Reynolds number was below 2000 for flow rates below 1.0 L/min. For pipe flow, laminar flow occurs when *Re* < 1000 while turbulent flow occurs when *Re* > 2000 (Faisst and Eckhardt, 2004). In the *Re* range between 1000 and 2000, laminar and turbulent flows are possible and are called "transition" flows.

In the TFF system, the fluid velocity is constant while it varies in the ATF system with a sinusoidal profile as schematically represented in Figure S1C. This sinusoidal profile has an absolute maximum value equal to the constant fluid velocity in the TFF. This implies that the instantaneous shear rate in the ATF system is sinusoidal as well, while it is constant in the TFF system. The shear rate in the ATF system can be written as

$$\gamma = \frac{\partial u}{\partial y} = \frac{\partial U_0 \sin(\omega t)}{\partial y} = \frac{\partial U_0}{\partial y} \cdot \sin(\omega t) \tag{S.5}$$

where ω is the frequency of the ATF cycle (s^{-1}), calculated from the flow rate of the ATF. The relationship between the ATF setting flow rate and the frequency can be expressed as

$$Q = 60 \cdot V \cdot \omega \tag{S.6}$$

where Q is the flow rate (L/min) in the hollow fiber cartridge filter and V (L) is the displacement volume of the ATF diaphragm pump, i.e. the chamber volume of the ATF.

In the range 0 to π, the average shear rate in the ATF can then be expressed as a function of its maximum absolute value constantly obtained in the TFF system, as follows

$$\gamma_{ATF} = \frac{\partial \mathrm{U}_0}{\partial \mathrm{y}} \cdot \frac{\int_0^{\pi} \sin(\omega t) \cdot d\omega t}{\pi} = \gamma_{TFF} \cdot \frac{2}{\pi} \approx 0.637\gamma_{TFF} \tag{S.7}$$

where $\frac{\partial U_0}{\partial y} = \gamma_{TFF}$ is the constant shear rate occurring in the TFF.
This result implies that the average absolute shear rate is lower in the ATF than in the TFF and is $\frac{2}{\pi} \approx 0.637$ of the average shear rate in the TFF, although the instantaneous shear rate in the ATF system has a maximum equal to the constant shear rate in the TFF system.
Taking into account **Eq**. S.3 and S.7, the average shear stress in the ATF, τ_{ATF}, can be written

$$\tau_{ATF} = \tau_{TFF} \cdot \frac{2}{\pi} \approx 0.637\, \tau_{TFF} \tag{S.8}$$

where τ_{TFF} is the average shear stress in the TFF.

Figure S.1D-E gives the shear rate and the shear stress as function of the flow rate in the ATF and TFF systems. For instance, for a flow rate of 1 L/min, the shear stress in the ATF and the TFF are 8.3 and 13 N/m^2, respectively, according to **Eq**. S.4.

A.2 Energy dissipation rate

The velocity profile equation for fully developed laminar flow in a pipe (Bird 2002, Brodkey 1995) is

$$\frac{dU_z}{dr} = \frac{-4Qr}{\pi R^4} \tag{S.9}$$

where Q is the volumetric flow rate, r is the radial position, and R is the radius of the pipe.
When the fluid is a Newtonian fluid and this equation can be derived to express the EDR, ϵ as

$$\epsilon = \sigma \left(\frac{dU_z}{dr}\right)^2 = \sigma \cdot \frac{16Q^2r^2}{\pi^2 R^8} \tag{S.10}$$

The value of $\frac{dU_z}{dr}$ is largest at the wall of the pipe, where $r = R$, so the maximum local EDR in this case is

$$\epsilon_{max} = \sigma \cdot \frac{16Q^2}{\pi^2 R^6} \tag{S.11}$$

Figure S.2A-B represents the EDR as function of the radius for different flow rates and the maximal EDR as function of the flow rate, given by **Eq**. S.11.

B METHODS

B.1 Generation of EPO-producing HEK293 cell line

A monoclonal HEK293F cell line expressing human recombinant erythropoietin (rhEPO) was created as follows. The gene encoding human EPO fused to a C-terminal HPC4-tag was cloned into the pD2529 expression vector (Atum) according to manufacturer's instructions (Electra cloning system). The plasmid was linearized by PvuI restriction enzyme. Freestyle 293-F cells (Gibco, Thermo Fisher Scientific) were cultured in Freestyle 293 expression medium (Gibco, Thermo Fisher Scientific) in 125 ml Erlenmeyer shake flask with vented caps at 37°C, 125 rpm and 8% CO_2. Cells were transfected at a cell density of 0.65 x 10^6 cells/ml with 1 µg of linearized plasmid per 1 million cells using PEI as transfection reagent at a DNA:PEI w/w ratio of 1:3 with. DNA and PEI were mixed by vortexing and precomplexed at 15 min before addition to cells. Isolation of stable plasmid-integrated clones was carried out by puromycin selection at a concentration of 2 µg/ml at day 2–13 post transfection. Single EPO-producing clones were isolated by sorting of single cells into each well of a 384-well plate using FACS (Astrios, Beckman Coulter) followed by verification of single cells by microscopy (Leica DMI6000B). Cells were expanded in Freestyle 293 medium supplemented with 1.5% HEPES at 37°C and 8% CO_2. A high-producing clone was identified by biolayer interferometry as described by Kol *et al* (Kol 2015) using CaptureSelect Biotin Anti-EPO Conjugate (Thermo Fisher Scientific) and the Octet RED96 instrument (Pall ForteBio, CA, USA).

B.2 Cell culture

The cells were routinely passaged every 3 or 4 day in CD-optiCHO medium (Thermo Fisher Scientific) in shake flasks (Corning) in a 5% CO_2 incubator. The medium was supplemented with 4 mM glutamine (Fujifilm Irvine Scientific), 100 mg/L streptomycin, 60 mg/L penicillin G (both Sigma-Aldrich) and puromycin (2 µg/mL) (Thermo Fisher Scientific).

B.3 Experimental setup

Bioreactor

The experiments were performed in four identical bioreactors of a DASbox Mini Bioreactor system (Eppendorf) equipped with marine impellers. The working volume in the bioreactor was 180 mL. The hold volume for the TFF system was 20 mL while it varied between 10 and 100 mL for the ATF system. The marine impellers had 3 cm diameter and were stirred at 250 rpm. The temperature was maintained at 37°C using a heating band. The pH was maintained at 7.0 using automatic additions of carbon dioxide or 0.5 M Na_2CO_3. The dissolved oxygen concentration (DO) was controlled at 40% air saturation using air, nitrogen and oxygen automatic additions. The cell density, viability, DO, pH, osmolality, and key nutrients and metabolites were daily monitored with a NovaBioprofile Flex (Nova Biomedical, USA).
The bioreactors were inoculated with cells at passage number between 6 and 24 at density 0.5 x 10^6 cells/mL, and the cell growth was monitored during 5 days. The reference condition was the absence of re-circulation in TFF or ATF, labeled 'No shear' in the graphs. This reference condition was carried out in triplicate, with cells at passages 6, passage 22 and passage 24.

Effect of shear stress

The effect of shear stress was studied by applying tangential flow filtration or alternating tangential flow filtration as used in perfusion culture, however the culture was carried out in batch mode for 5 days. For this, the TFF and ATF were connected in the same way as these are connected for perfusion operation but no fluid was removed from the permeate side of the hollow fiber. The HF cartridge of the ATF was connected to the bioreactor with a dip tube. The same connection was

used for the TFF system where the cell broth was recycled to the bioreactor using another dip tube connection in the bioreactor head plate. In both the ATF and TFF systems, the tangential flow filtration was performed using hollow fiber cartridges (GE Healthcare - Cytiva, CFP-4-E-3MA with 13 fibers, membrane area 110 cm^2, pore size 0.45 μm, fiber lumen 1 mm, nominal low path length 30 cm). The schematic setups for TFF and ATF are shown in **Figure 1**.

ATF system

In the ATF system, the diaphragm pump of an ATF-2 device (Repligen, Refine Technology) generated an alternating flow recirculation in the HF. The operating conditions for ATF were $0.2_{(n=1)}$, $0.3_{(n=1)}$, $0.4_{(n=1)}$, $0.5_{(n=1)}$, $0.6_{(n=2)}$, $0.7_{(n=3)}$, $0.8_{(n=2)}$, $0.9_{(n=3)}$ and $1_{(n=1)}$ L/min (shear stress 1.6-7.5 N/m^2), with absence of recirculation 'No shear' as control condition, i.e. $0_{(n=3)}$ L/min, where subscript n denotes the number of repetitions per condition.

TFF system

In the TFF system, the flow was driven in one direction by a peristaltic pump Alitea XV (Watson-Marlow) for flow rate ≤ 0.38 mL/min. For this system, the pump tube was a GORE STA-PURE PCS pump tube 3/16'' ID x 5/16'' OD made of silicone in a PTFE lattice (ePTFE and platinum-cured silicone composite – Gore) or a PharMed BPT pump tube 3/16'' ID x 5/16'' OD (Saint-Gobain) in preliminary studies as detailed in the text. This pump had an operating range up to 0.19 L/min, hence to obtain a flow of 0.38 mL/min, two pumps were used in parallel and above that flow the diaphragm pump of the ATF2 system was used in combination with one-way check valves to create a flow in one direction. The operating conditions for TFF were $0.127_{(n=1)}$, $0.191_{(n=2)}$, $0.38_{(n=2)}$, $0.5_{(n=2)}$ and $0.7_{(n=2)}$ L/min (shear stress 1.6-9.1 N/m^2), with the same control conditions as ATF, i.e. $0_{(n=3)}$ L/min absence of recirculation 'No shear'.

B.4 Metabolism and product analyses

The cell growth and main metabolite concentrations were daily measured to monitor the metabolic production and consumption rates. The viable cell density, viability and concentrations of the main metabolites, glucose, lactate, glutamine and ammonia, were analyzed by Bioprofile Flex (Nova Biomedical, USA). Amino acid analysis was performed based on a Waters UPLC Amino Acid Analysis applications kit using the vendor's protocol; briefly: Cell culture supernatants were filtered through 10 kDa filters and filtrates were diluted using HPLC grade water to appropriate concentrations. Amino Acid Standard (Waters) was diluted for use as a standard curve. Diluted samples and standards were combined with internal standard Norvaline (Sigma-Aldrich) and AccQ Tag Derivatization Kit reagents (Waters). Samples were run on an Acquity UPLC system (Waters) using an AccQ-Tag Ultra RP Column 130 Å 1.7 µm, 2.1 mm, 100 mm (Waters). Data were analysed using EMPOWER software (Waters). Recombinant human erythropoietin (rhEPO) expressed by HEK293 was quantified using a sandwich ELISA kit (Invitrogen) with human erythropoietin Standard used as standard.

The cell growth rate μ_i at time $T_{i\ (i=1,\dots,5)}$ was calculated as follows

$$\mu_i = \frac{\ln\left(C_{tot_i}/C_{tot_{i-1}}\right)}{T_i - T_{i-1}} \tag{S12}$$

where C_{tot_i} is the total cell density (x 10^6 cells/mL) at time T_i.
The cell specific consumption rate of a substrate *c*, q_{c_i}, (e.g. glucose) at time T_i was calculated as

$$q_{c_i} = \frac{2\left(C_{i-1} - C_i\right)}{\left(T_i - T_{i-1}\right)\left(C_{v_i} + C_{v_{i-1}}\right)} \tag{S13}$$

where C_i is the concentration of the metabolite *c*, and C_{v_i} the cell density at time T_i.
The cell specific production rates of a product *p* (e.g. lactate, rhEPO) at time T_i, q_{p_i}, was calculated as:

$$q_{p_i} = \frac{2\ (P_i\ - P_{i-1})}{(T_i - T_{i-1})\ (C_{v_i} + C_{v_{i-1}})} \quad \text{(S14)}$$

where P_i *is* the concentration of product *p*.

For the calculation of the growth rate, as well as the cell specific consumption of glucose and production of lactate, weighted moving averaging was applied on the data. The average $\bar{x}_i$ calculated as:

$$\bar{x}_i = \frac{x_{i-1} + 2\,x_i + x_{i+1}}{4} \quad \text{(S15)}$$

was considered for **Eq S12, S13** and **S14**, where $x_{i\ (i=1,\dots,5)}$ was the cell density, the glucose concentration or the lactate concentration at sampling events T_i . The average of the specific rates at day 2 and at day 3, where exponential growth occurred, was considered.

Statistical comparisons of the metabolic rates were made using Student's t-test for unpaired samples and unequal sample sizes according to Cardillo 2006. p-values < 0.05 were considered significant and are given in the text.

B.5 RNA sample preparation and transcript profiling of HEK293 cells

For RNA extraction, 1 mL cell broth samples were collected from the bioreactors on a daily basis, centrifuged at 4°C and the cell pellet was resuspend in 200 µL RNAlater Stabilization Solution (Invitrogen, Thermo Fisher Scientific) to stabilize and preserve the cells. These were then kept at 4°C overnight and then stored at -80°C until analysis. Frozen pellets were thawed and subsequently treated as starting material for Total RNA extraction and analysis. Briefly, cells were lysed and homogenized, followed by genomic DNA removal on gDNA Eliminator spin columns and RNA Isolation on RNeasy® Spin Columns utilizing the Qiagen RNeasy® Plus Universal Mini Kit according to manufacturer's instructions (Qiagen, Germany). Quality control on extracted Total RNA prior to sequencing was performed on an Agilent Bioanalyzer 2100 system together with the Agilent RNA 6000 Nano kit (Agilent Technologies, CA, US). All samples submitted for sequencing had a RNA Integrity number (RIN) >8. They were sequenced using Illumina HiSeq 2500 High Output Mode, at paired-end 2x125bp (Illumina HiSeq platform via a commercial service of Eurofins MWG GmbH, Germany). Subsequently, we processed FASTQ files as paired-end raw sequencing data and quantify TPM and count values for transcripts by Kallisto method (Bray 2016) using cDNA human reference (GRCh38) from Ensembl release 92. We added the transcript sequence of recombinant EPO to the reference FASTA file to investigate the expression of recombinant EPO in different flow/shear rate. The gene count and TPM values were calculated from transcript level abundance and counts using R package tximport (Soneson 2015) based on Ensembl gene version 92.

B.6 Clustering Similarity Matrices, correlation, differential expression and statistical analyses

The similarity matrix for the samples were generated based on Spearman correlation regarding the log transformed TPMs. We used Hierarchical clustering with Ward.D2 and Euclidean distance to cluster the samples based on the similarity matrix.
Differential expression analyses were performed based on raw counts through R using the DESeq2 package and Wald test p value (Love 2014). Differential expression analysis was performed by

partitioning subjects according to either different bioreactor system or high *vs.* low shear rate. Genes displaying median TPM value <1 across samples were ignored.
Hypothesis testing was performed by considering the null hypothesis of absence of association between the compared variables. The statistical test for association was selected according to the nature of the data: continuous data *vs.* continuous data by Spearman rank correlation test and categorical data *vs.* categorical data by Fisher's exact test for 2x2 tables. Statistical methods are indicated and considered significant after multiple hypothesis testing (Benjamin-Hochberg) where Q < 0.05. Spearman rank correlations were computed for gene expression *vs.* cultivation parameters across samples, and Q values were used to find significant correlations as indicated throughout. Cytoscape (Shannon 2003) was used to visualize the co-expression network.

B.7 Gene set enrichment and KEGG pathway analysis

Gene set enrichment analysis (GSEA) was performed through PIANO using whole-genome Log_2 fold changes and adjusted P values attained from DESeq2 as gene-level statistics, with geneSetStat = reporter, and nPerm = 1000. Gene Ontology biological processes were downloaded from MSigDB (Liberzon 2014). Gene Ontology processes were considered as enriched with an FDR of 5%, and with clear direction (i.e. non-mixed). Additionally, we ignored Gene Ontology processes related with tissues/organs of different embryonic origin (e.g. brain, bone, hair).
Gene expression enrichment was also performed on KEGG metabolic pathways through PathWave (Schramm 2010), with 1000 permutations. Local pathways were selected if at least three reactions (or genes) were enriched in a pathway (Q < 0.05). The inputs of PathWave were TPM values for the genes having Entrez ID and the median TPM>1. For ID mapping the "org.Hs.eg.db" R package was used (Carlson 2019).

B.8 Data availability

The data are available at doi:10.17632/bb5vw384h3.1 (Mendeley data).

SUPPLEMENTAL REFERENCES

Bird, R.B. (2002), *Transport phenomena*. Applied Mechanics Reviews 55, R1-R4.

Bray, N.L., Pimentel, H., Melsted, P., Pachter, L., 2016. Near-optimal probabilistic RNA-seq quantification. Nat Biotechnol. 34(5):525-7. doi: 10.1038/nbt.3519. Epub 2016 Apr 4.

Brodkey, R.S. (1995) *The phenomena of fluid motions*. Courier Corporation.

Cardillo, G. (2006). Student t-Test for unpaired or paired samples. http://www.mathworks.com/matlabcentral/fileexchange/12699

Carlson, M., 2019. org.Hs.eg.db: Genome wide annotation for Human. R package version 3.8.2

Cross Flow Filtration Method Handbook, 29-0850-76 AB 03/2014 a1675, GE Healthcare

Faisst, H. and Eckhardt, B. (2004). Sensitive dependence on initial conditions in transition to turbulence in pipe flow. Journal of Fluid Mechanics 504, 343-352.

Liberzon A., 2014. A description of the Molecular Signatures Database (MSigDB) Web site. Methods Mol Biol. 1150:153-160. doi:10.1007/978-1-4939-0512-6_9

Love, M.I., Huber, W. and Anders, S., 2014. Moderated estimation of fold change and dispersion for RNA-seq data with DESeq2. Genome Biol. 15(12):550. PMID: 25516281, PMCID: PMC4302049

Schramm, G., Wiesberg, S., Diessl, N., Kranz, A.L., Sagulenko, V., Oswald, M., Reinelt, G., Westermann, F., Eils, R., König, R., 2010. PathWave: discovering patterns of differentially regulated enzymes in metabolic pathways. Bioinformatics. 1;26(9):1225-31. doi: 10.1093/bioinformatics/btq113. PMID: 20335275

Selection Handbook, Hollow fiber cartridges and systems for membrane separations, 18-1165-29 AC, GE Healthcare

Shannon, P., Markiel, A., Ozier, O., Baliga, N.S., Wang, J.T., Ramage, D., Amin, N., Schwikowski, B., Ideker, T., 2003. Cytoscape: a software environment for integrated models of biomolecular interaction networks. Genome Res. 13(11):2498-504. PMID: 14597658, PMCID: PMC403769

Soneson C., Love. M.I., Robinson, M.D. Differential analyses for RNA-seq: transcript-level estimates improve gene-level inferences. *F1000Res*. 2015;4:1521. doi:10.12688/ f1000research. 7563.2

Väremo, L., Nielsen, J., Nookaew, I., 2013. Enriching the gene set analysis of genome-wide data by incorporating directionality of gene expression and combining statistical hypotheses and methods. Nucleic acids research 41(8): 4378-4391